



# Optics Letters

## Atomic coherence-assisted wide tunable range laser frequency offset locking using four-wave mixing

JUN GUO,<sup>1,†</sup> ZHENG TAN,<sup>1,2,†</sup> KEXIANG MOU,<sup>1</sup> LI WANG,<sup>1,2</sup> YINAN HU,<sup>1,2</sup> XIANPING SUN,<sup>1,2</sup> AND XIN ZHOU<sup>1,2,\*</sup>

<sup>1</sup>State Key Laboratory of Magnetic Resonance Spectroscopy and Imaging, Innovation Academy for Precision Measurement Science and Technology, Chinese Academy of Sciences – Wuhan National Laboratory for Optoelectronics, Huazhong University of Science and Technology, Wuhan, 430071, China

<sup>2</sup>University of Chinese Academy of Sciences, Beijing 100049, China

<sup>†</sup>These authors contributed equally to this work.

\*xinzhou@wipm.ac.cn

Received 8 October 2024; revised 2 March 2025; accepted 4 March 2025; posted 4 March 2025; published 28 March 2025

**In this Letter, we present a widely tunable laser frequency offset locking technique based on four-wave mixing (FWM). The Raman-amplified probe light and newly generated conjugate light exhibit high signal amplitude and ultra-narrow spectral characteristics, which contribute to robust laser frequency stabilization. The laser frequency can be selectively locked to the Stokes or anti-Stokes frequency of the four-wave mixing spectrum, maintaining a fixed frequency difference relative to the pump light that corresponds to the atomic ground state hyperfine splitting. By adjusting the detuning of the pump light frequency, a wide tuning range of several GHz can be achieved. Compared to the frequency modulation spectroscopy method, the modulation transfer technique in a double-lambda atomic system provides an atomic coherence-enhanced error signal with a larger peak-to-peak amplitude and a steeper zero-crossing gradient, resulting in significantly improved laser frequency stabilization performance. This method can enhance the performance of atomic sensors, such as improving the stability of the Raman light for atomic interferometers and increasing the laser stability of highly sensitive atomic magnetometers.**

© 2025 Optica Publishing Group. All rights, including for text and data mining (TDM), Artificial Intelligence (AI) training, and similar technologies, are reserved.

<https://doi.org/10.1364/OL.543109>

Laser frequency stabilization is vital in various atomic physics experiments, particularly in the field of precision measurements. Various techniques have been employed to derive error signals that can be used to lock the laser frequency to a stable reference frequency. The most commonly used method is to reference laser frequencies to atomic transitions. Existing laser frequency stabilization techniques can be classified into two main types: modulated schemes, such as saturated absorption spectroscopy (SAS), frequency modulation spectroscopy (FMS) [1,2], modulation transfer spectroscopy (MTS) [3,4], and Pound–Drever–Hall (PDH) [5], and unmodulated schemes, such

as dichroic atomic vapor laser lock (DAVLL) [6–8], a combination of DAVLL and saturated absorption [9,10], Sagnac interferometry [11], and polarization spectroscopy [12].

In some atomic physics experiments, maintaining a fixed frequency difference between two lasers is more important than the absolute frequency stabilization of a single laser. A two-laser system is commonly used for laser offset frequency locking by employing pump–probe spectroscopy in a three-level atomic system. For example, in electromagnetically induced transparency (EIT) [13–15], the sub-natural two-photon resonance provides the frequency reference to lock the frequency difference of two lasers to the atomic ground state hyperfine splitting. However, the tuning range of the frequency offset locking for EIT is limited to several hundred MHz due to the restricted Doppler width of the atoms and laser interactions [16]. The beat signal of the two lasers with a specific frequency difference is also used as the locking error signal; however, high-frequency electronics are typically required [17]. Using an acousto-optic modulator (AOM) allows for the tunability of off resonance frequency locking; however, it is still limited by the modulation bandwidth and noise of the external modulator. In conventional pump–probe FMS locking schemes, such as SAS and MTS, the frequency stability is limited by the stability of the pump laser because the noise of the pump laser is transferred to the frequency noise power of the locking system, thereby diminishing the locking performance of the probe laser.

In light–atom interaction experiments, off resonance locking is usually required, such as the detuned probe laser in atomic magnetometry [18,19] and quantum light sources for atomic sensing [20]. Stabilizing the relative frequency difference between two independent lasers can be advantageous in some applications, such as the application of Raman light in atomic interference [21,22] and Raman sideband cooling atoms to the ground state [23,24].

In this Letter, we present a laser frequency offset locking technique using four-wave mixing (FWM) based on atomic coherence and quantum interference effects [25]. The FWM system offers a sub-natural-linewidth reference signal and a large frequency-tunable range over several GHz off resonance from atomic transitions. Moreover, by combining MTS with the FWM

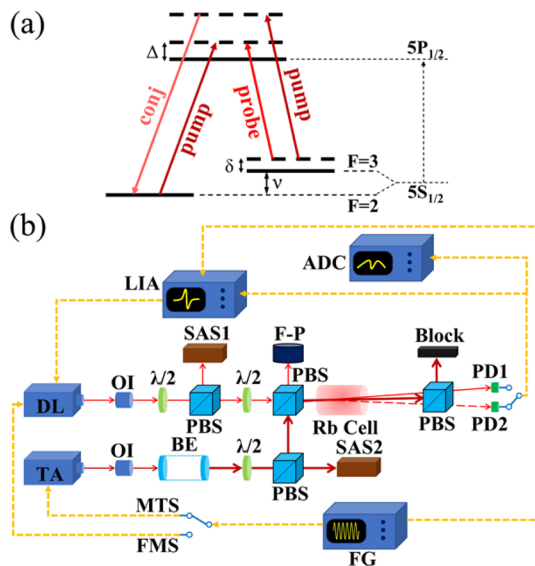


**Fig. 1.** Energy-level diagram and experimental setup for the ACA-MTS laser frequency locking. (a) Double-lambda system in the  $^{85}\text{Rb}$  D<sub>1</sub> line transition. (b) Laser frequency-locking setup based on FWM. OI, optical isolator;  $\lambda/2$ , half-wave plate; BE, beam expander; PBS, polarization beam splitter; SAS, saturated absorption spectroscopy; F-P, Fabry-Perot interferometer; LIA, lock-in amplifier; DL, tunable diode laser; TA, tapered amplifier laser; PD, photodetector; FG, function generator.

system, a locking error signal with a much larger peak-to-peak amplitude and a steeper zero-crossing gradient was obtained compared with the result obtained using conventional FMS. This technique is named atomic coherence-assisted modulation transfer spectroscopy (ACA-MTS). By frequency modulating the pump laser while demodulating the detection signal of the probe laser, the frequency and amplitude noise introduced by directly modulating the probe laser can be effectively avoided. Furthermore, in our experiment, the performance of the ACA-MTS method was significantly better than that of the FMS method and was not dependent on the stability of the pump laser due to the atomic coherence generated in the FWM process. This is different from absorption-based locking schemes, such as SAS [13]. Similar to conventional MTS in a two-level atomic system, ACA-MTS also exhibits a zero background near the locking frequency, making it immune to environmental fluctuations. Therefore, highly stable frequency-locking performance can be achieved due to the enhanced locking error signal obtained by utilizing atomic coherence in the FWM medium.

The energy-level diagram used is shown in Fig. 1, where FWM is generated in a three-level atomic system, forming a double-lambda configuration. The  $5S_{1/2}$   $F=2$  or  $3 \rightarrow 5P_{1/2}$  transition of the  $^{85}\text{Rb}$  atom is chosen; two separate lasers are used as a pump light and a probe light, respectively; and their frequency difference is set to match the atomic ground state energy-level interval to generate the FWM process. The pump laser couples the hyperfine ground state  $5S_{1/2}$ ,  $F=2$  and excited state  $5P_{1/2}$  with detuning  $\Delta$ , while the probe laser couples the state  $5S_{1/2}$ ,  $F=3$  and the same excited state, satisfying the two-photon resonant ( $\delta=0$ ) with pump laser frequency.

The experimental setup is depicted in Fig. 1(b). The tunable external cavity diode laser (TOPTICA), with a mode-hop-free tunable range of approximately 30 GHz and a laser power of

$500 \mu\text{W}$ , operates as the probe light. A tapered amplifier laser (TA) (TOPTICA) with a power output of approximately 300 mW was used as the pump light. The polarizations of the two lights were orthogonal. A cylindrical rubidium atomic vapor cell with a diameter of 10 mm and a length of 30 mm was used as the FWM medium. During the experiment, the temperature of the rubidium vapor cell was controlled at about  $120^\circ\text{C}$  using a PID controller. The beam diameter of the pump light was expanded to 5 mm by a beam expander (BE) before entering the rubidium vapor cell to ensure good spatial overlap with the probe light. The probe light, with a beam diameter of 3 mm, entered the rubidium vapor cell, where it co-propagated with the pump light at an overlapping angle of approximately 6 mrad. When the phase-matching condition was satisfied, the FWM process occurred via the third-order nonlinear susceptibility of the atomic medium. After passing through the vapor cell, the pump light was separated by the polarization beam splitter (PBS) due to its orthogonal polarization to the probe light. Due to the incident angle of the probe and pump lights, the amplified probe light and the newly generated conjugate light are distributed on both sides of the pump light. After spatial separation, the two lights are detected by photodetectors (PDs) PD1 and PD2, respectively.

In our experiment, the MTS method was adopted to obtain the dispersive error signal for probe laser locking. In this method, the pump light frequency is modulated, while the probe light signal is demodulated before being fed back to the laser. As shown in Fig. 1(b), by switching the modulation channel, laser frequency-locking methods based on FMS and MTS can be selected, allowing for a comparison of their frequency-locking results.

To obtain the FWM spectrum of rubidium atoms, the pump light frequency is adjusted to be blue-detuned by  $\sim 1$  GHz from the  $^{85}\text{Rb}$   $F=2 \rightarrow F'=3$  transition, while the probe light frequency is simultaneously scanned  $\sim 12$  GHz across the  $^{85}\text{Rb}$  D<sub>1</sub> line transition. The rubidium vapor cell is heated to maintain an atomic density of  $\sim 10^{14} \text{ cm}^{-3}$ . As a frequency reference, the absorption and saturated absorption spectra of Rb atoms are shown in Fig. 2(a). By scanning the probe light frequency, it is observed that the probe light is optically amplified, and a conjugate light with a new frequency is generated through the FWM process. Their frequency difference matches twice the ground state energy-level separation, as shown in Figs. 2(b) and 2(c). The probe light gain is related to parameters such as the phase-matching angle, pump light intensity, and temperature of the atomic vapor. With the optimized experimental parameters, amplification of the probe light can be realized several dozen times. Figure 2(c) shows the signal from PD2, which corresponds to the newly generated conjugate light in the FWM process. The spectrum has a clean baseline and crosses the zero character; therefore, it is suitable as the source of the error signal for laser locking. In the insets of Fig. 2, the error signals obtained using the FMS method by modulating the probe laser current (0.15 mA modulation amplitude and 3.2 kHz modulation frequency) are shown.

The off resonance frequency tunability of FWM makes it suitable for realizing large tunable range-frequency offset locking. When the pump light frequency is continuously adjusted to approximately 6 GHz, the signal transmission can be clearly seen. The energy level of the  $^{85}\text{Rb}$  atomic level is used to demonstrate the frequency offset locking in this work; the offset locking tuning range can be further expanded up to more than 10 GHz

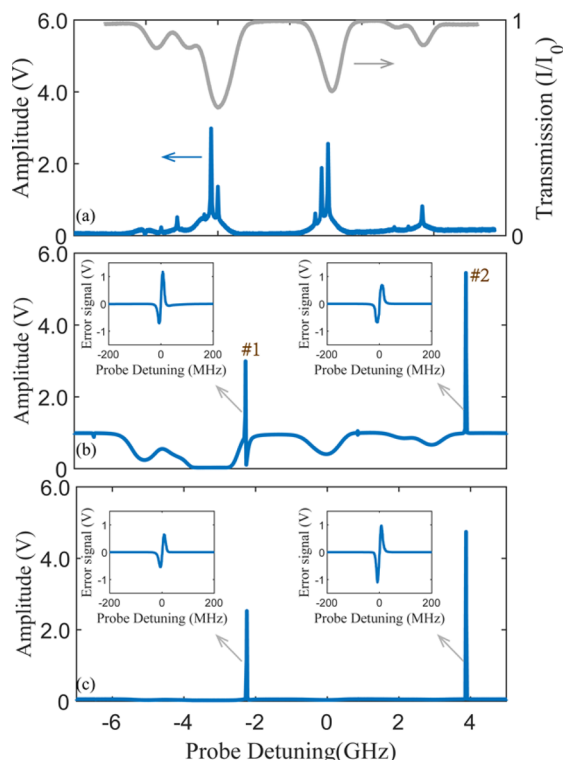


**Fig. 2.** (a) Absorption spectrum and the saturated absorption spectrum of natural rubidium atoms. The zero-frequency point in the  $x$  axis corresponds to  $F = 2 \rightarrow F' = 3$  of the  $^{85}\text{Rb}$   $D_1$  line transition. The transmitted signal amplitude of the (b) probe light and (c) conjugate light as varying the probe detuning; the pump light frequency is blue-detuned to about 1 GHz, representing the single-photon detuning  $\Delta$ . In (b), the position of #1 peak and #2 peak represent the frequencies of the amplified probe light and the newly generated conjugate light, respectively. The insets show error signals obtained by the probe light and the conjugate light by the FMS method.

by combining the  $^{87}\text{Rb}$  transitions, which indicates the excellent tunability of the FWM-based frequency-locking method.

For the ACA-MTS locking scheme, we used the modulation transfer technique to generate an error signal for frequency offset locking and a dispersive line-shaped signal with a flat, zero background, similar to the MTS in the two-level atomic system. However, in this study, we demonstrate that the modulation transfer in the FWM medium significantly increases the amplitude and gradient of the error signal, greatly enhancing laser frequency stabilization. The pump light was modulated at a frequency of 5.01 kHz with an amplitude of 0.027 mA, and the modulation signal was fed into the LIA to demodulate the detected probe light signal. In the experiment, the power ranges of the pump light and the probe light were 150 mW–650 mW and 10  $\mu\text{W}$ –500  $\mu\text{W}$ , respectively, and effective locking error signals can be obtained within these ranges. For comparison, we also obtained an error signal using the FMS method with the same modulation parameters (amplitude and frequency).

As shown in Fig. 3(a), for the error signal obtained from the probe light, the gradient of the FMS signal is 0.05 V/MHz, while the gradient of the ACA-MTS signal is 0.13 V/MHz. Figure 3(b) shows the error signal from the conjugate light, where the gradient of the FMS signal is 0.08 V/MHz, and the

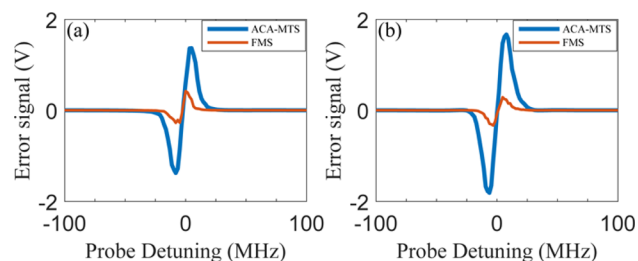


**Fig. 3.** Error signals obtained from the (a) probe light and (b) conjugate light for the FMS and the ACA-MTS methods under the same modulation parameters, respectively. The red (thinner) line corresponds to the result with the FMS method, while the blue (thicker) one corresponds to the enhanced error signal using the ACA-MTS method.

gradient of the ACA-MTS signal is 0.25 V/MHz. By modulating the pump light, the large nonlinearity generated in the FWM medium results in a significantly greater amplitude of the error signal than that obtained by directly modulating the probe light. This can be understood as a parametric amplification effect assisted by atomic coherence in the double-lambda atomic configuration [13,26,27]. It is evident that the amplitude and gradient enhancement of the newly generated conjugate light are more conspicuous. The enlarged ACA-MTS signal appeared over the entire pump light tuning range for the FWM process. The ACA-MTS method effectively reduces the frequency drift introduced by the direct modulation of the probe light, thereby greatly improving the stability of laser frequency locking.

To demonstrate the advantage of the atomic coherence-enhanced MTS method, the locking performances of the ACA-MTS and conventional FMS methods under the same experimental parameters were investigated. Figure 4 shows the frequency fluctuation of the frequency-offset-locked laser under the conditions of the ACA-MTS, FMS, and free-running, measured using a Fabry–Perot interferometer (F–P) shown in Fig. 1(b). In the case of free-running laser, the frequency fluctuation at 600 s is approximately 8 MHz. When the probe light is locked using the FMS method, the frequency fluctuation is  $\pm 2.25$  MHz. Using the ACA-MTS approach, the pump laser is stabilized at the  $^{85}\text{Rb}$   $F = 2 \rightarrow F' = 3$  transition by the SAS method. The modulation is transferred to the probe light through the nonlinear FWM process, and the demodulated error signal is used to lock the probe laser, achieving a frequency fluctuation of  $\pm 0.53$  MHz. The inset of Fig. 4 shows the noise spectrum of the probe light via the fast Fourier transform (FFT) for the FMS and ACA-MTS locking methods. The stability of the frequency-offset-locked laser was analyzed based on the Allan deviation as well. By measuring the beat note frequency using another independent external cavity diode laser, the frequency stability of the laser was estimated to be  $5.46 \times 10^{-12}$  using the FMS method and  $1.94 \times 10^{-12}$  using the ACA-MTS method with an averaging time of 400 s, as illustrated in Fig. 5. Therefore, modulation signals of the same amplitude and frequency demonstrate the superior locking performance of the ACA-MTS method, which presents a better frequency stability and lower noise levels than that of the FMS method.

In conclusion, we have demonstrated a wide-tunable range laser frequency offset locking technique assisted by atomic coherence in an FWM medium, which can achieve a large off-resonance tuning range of several GHz relative to a specific atomic

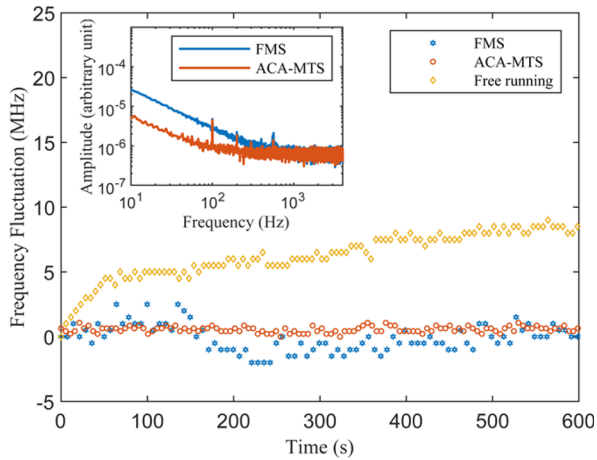


**Fig. 4.** Frequency fluctuations for the free-running, FMS, and ACA-MTS methods in continuous running for 10 min. Compared to the laser free running and the FMS locking, the frequency fluctuation for the ACA-MTS locking is greatly suppressed. The inset shows the noise spectrum of the probe light by FFT for the FMS and ACA-MTS locking methods, respectively.

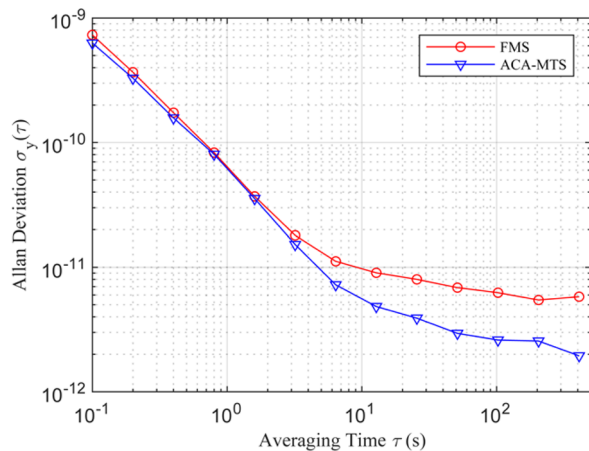


**Fig. 5.** Allan deviation for the frequency stability of the frequency-offset-locked laser using the FMS and ACA-MTS methods.

transition. By combining MTS in the FWM process, we found that the ACA-MTS approach enables much larger peak-to-peak amplitude and a steeper zero-crossing gradient of the error signal compared with the conventional FMS method, which allows for much better laser frequency-locking stability. In this study, the error signal was fed back to the piezo to compensate for the cavity length at a low speed. Therefore, better locking performance can be expected if high-speed current feedback is used simultaneously. Furthermore, the offset-locked laser system provides two light sources with a stable frequency difference, which can enhance the measurement sensitivity and stability of atomic sensors. In particular, the ACA-MTS method can be used to produce stable quantum light sources, with potential applications in quantum sensing for extracting weak signals from a noisy

background [28,29]. In addition, by selecting either the probe light or conjugate light as the source of the error signal, the frequency-locking point can be switched between the Stokes and anti-Stokes frequencies, which are separated by twice the ground state energy-level splitting. This capability could enhance the background noise rejection of multichannel narrow-bandwidth optical filters [30,31] for free-space optical communications and lidar systems for remote atmospheric wind measurement [32].

**Funding.** National Key R&D Program of China (2023YFF0714000); Scientific Instrument Developing Project of the Chinese Academy of Sciences (YJKYYQ20210044).

**Disclosures.** The authors declare no conflicts of interest.

**Data availability.** The data underlying the results presented in this Letter are not publicly available at this time but may be obtained from the authors upon reasonable request.

## REFERENCES

- J. Mandon, G. Guelachvili, and N. Picqué, *Opt. Lett.* **32**, 2206 (2007).
- K. Szymaniec, S. Ghezali, L. Cognet, *et al.*, *Opt. Commun.* **144**, 50 (1997).
- J. H. Shirley, *Opt. Lett.* **7**, 537 (1982).
- C. So, N. L. R. Spong, C. Möhl, *et al.*, *Opt. Lett.* **44**, 5374 (2019).
- Z. Wang, H. Wei, Y. Li, *et al.*, *Opt. Lett.* **45**, 1148 (2020).
- K. L. Corwin, Z.-T. Lu, C. F. Hand, *et al.*, *Appl. Opt.* **37**, 3295 (1998).
- D. J. McCarron, I. G. Hughes, P. Tierney, *et al.*, *Rev. Sci. Instrum.* **78**, 1 (2007).
- S. Pustelny, V. Schultze, T. Scholtes, *et al.*, *Rev. Sci. Instrum.* **87**, 1 (2016).
- M. Himsforth and T. Freearge, *Phys. Rev. A* **81**, 023423 (2010).
- J. Zhang, D. Wei, C. Xie, *et al.*, *Opt. Express* **11**, 1338 (2003).
- G. Jundt, G. T. Purves, C. S. Adams, *et al.*, *Eur. Phys. J. D* **27**, 273 (2003).
- C. P. Pearman, C. S. Adams, S. G. Cox, *et al.*, *J. Phys. B: At. Mol. Opt. Phys.* **35**, 5141 (2002).
- A. W. Brown and M. Xiao, *Phys. Rev. A* **70**, 053830 (2004).
- R. P. Abel, A. K. Mohapatra, M. G. Bason, *et al.*, *Appl. Phys. Lett.* **94**, 071107 (2009).
- S. C. Bell, D. M. Heywood, J. D. White, *et al.*, *Appl. Phys. Lett.* **90**, 1 (2007).
- M. Parniak, A. Leszczyński, and W. Wasilewski, *Appl. Phys. Lett.* **108**, 1 (2016).
- L. Gianfrani, A. Castrillo, E. Fasci, *et al.*, *Opt. Express* **18**, 21851 (2010).
- M. Zhu, L. Wang, J. Guo, *et al.*, *Opt. Express* **29**, 28680 (2021).
- W. Xiao, X. Liu, T. Wu, *et al.*, *Phys. Rev. Lett.* **133**, 093201 (2024).
- S. Wu, G. Bao, J. Guo, *et al.*, *Sci. Adv.* **9**, eadg1760 (2023).
- S.-w. Chiow and N. Yu, *Appl. Phys. B* **124**, 96 (2018).
- M. F. Locke and Y. H. Shih, *Phys. Rev. A* **103**, L031303 (2021).
- H. Alaeian and M. S. Shahriar, *Phys. Rev. A* **97**, 053829 (2018).
- Y. Lu, S. J. Li, C. M. Holland, *et al.*, *Nat. Phys.* **20**, 389 (2024).
- Z. Qin, J. Jing, J. Zhou, *et al.*, *Opt. Lett.* **37**, 3141 (2012).
- Y. Zhu, *Phys. Rev. A* **55**, 4568 (1997).
- K.-i. Takahashi, N. Hayashi, H. Kido, *et al.*, *Phys. Rev. A* **83**, 063824 (2011).
- L. E. E. de Araujo, Z. Zhou, M. DiMario, *et al.*, *Opt. Express* **32**, 1305 (2024).
- M. Guo, H. Zhou, D. Wang, *et al.*, *Phys. Rev. A* **89**, 033813 (2014).
- Z. Tan, X. Sun, J. Luo, *et al.*, *Chin. Opt. Lett.* **9**, 021405 (2011).
- X. Zhao, X. Sun, M. Zhu, *et al.*, *Opt. Express* **23**, 17988 (2015).
- C. Nagasawa, Y. Shibata, M. Abo, *et al.*, *Proc. SPIE* **4153**, 338 (2001).